

SYNCHROTRON RADIATION AND ITS POLARIZATION FROM RUNAWAY ELECTRONS IN TOROIDAL MAGNETIC FIELDS

Ya.M. Sobolev

Institute of Radio Astronomy NASU, Kharkov, Ukraine

E-mail: sobolev@rian.kharkov.ua

The formulas to describe synchrotron radiation and its polarization in toroidal magnetic field configurations are presented. The radiated power and direction of polarization of the synchrotron radiation spot of runaway electrons for medium-sized tokamaks are estimated. Two polarization models are proposed. It is shown that the polarization measurements give additional diagnostics for the radiating relativistic electrons.

PACS: 41.60.Ap, 52.55.Fa, 97.60.Gb

INTRODUCTION

Synchrotron radiation provides information about the runaway electrons in tokamaks. Polarization measurements will give extra features.

In [1] the formulas that take into account curvature of magnetic field lines have been derived. In [2 - 4] the radiation formulae of a relativistic charge moving along bent spiral path have been generalized. The new expressions for frequency spectra and polarization components of synchrotron radiation were obtained. The synchrotron radiation spectrum of runaway electrons in tokamak was received in [5].

In [6] the polarization pattern of the synchrotron radiation of runaway electrons in tokamak has been calculated.

The synchrotron radiation is the powerful tool to diagnose the parameters of relativistic runaway electrons. This diagnostic provides a direct image of the runaway beam inside the plasma. The radiation was measured in infra-red and visual wavelength ranges [7 - 10].

Analysis of experimental data has shown that the description of the synchrotron radiation of runaway electrons in tokamaks is the case when you need to take into account the curvature of magnetic field lines.

In this paper, we will continue to study the polarization of synchrotron radiation in a toroidal magnetic field configuration, using formulas from [3, 6].

The topology of toroidal magnetic fields and drift trajectories, the electron energies take values that are typical for medium-size tokamaks.

The paper is organized as follows. The formulas proposed to describe the synchrotron radiation are given in Section 1. Terms of using these formulas instead of classical formulas of synchrotron radiation are written out.

In Section 2, the spectrum and polarization properties of radiation emitted by relativistic electrons are derived. The formulas for calculating the direction of polarization are given. The contribution to the radiation in the defined direction from one or two emitting points is considered.

In Section 3, the polarization in synchrotron radiation spot is calculated and discussed. The influence on the polarization pattern of unequal shift of drift trajectories is shown.

1. RADIATION FORMULAE IN CURVED MAGNETIC FIELDS

The spectral power density of the synchrotron radiation emitted by relativistic electrons moving within magnetic field lines with curvature radius R_B and magnetic field B is expressed by [3, 4]

$$\frac{dP_i}{d\lambda} = \frac{P_C}{\lambda_C} f_i(y_C, q_a), \quad (1)$$

$$f_i(y_C, q_a) = \frac{9\sqrt{3}}{16\pi} y_C \left\{ \int_{\frac{y_C}{|1-q_a|}}^{\infty} dx F_i(x) + \frac{1}{\pi} \int_{\frac{y_C}{1+q_a}}^{\frac{y_C}{|1-q_a|}} dx F_i(x) \left(\frac{\pi}{2} + \arcsin \frac{1+q_a^2 - y_C^2/x^2}{2q_a} \right) \right\}$$

here $P_C = \frac{2}{3} \frac{e^2}{c} \gamma^4 \beta_{\parallel}^2 \Omega^2$ is the total power emitted by a charged particle moving with velocity V_{\parallel} along a circular orbit of radius R_B , $y_C = \lambda_C/\lambda$, $\lambda_C \approx 4\pi/(3\gamma^3\Omega)$ the characteristic radiation wavelength, $\Omega = V_{\parallel}/R_B$, $q_a = \omega_B^2 r_B / (\Omega^2 R_D)$, $\omega_B = eB/(\gamma mc)$, $e = |e|$, m , γ are the electron charge, mass, and Lorentz-factor, r_B is the Larmor radius, $i = \pi, \sigma$ denote the cases of π - and σ -polarization,

$$F_{\pi} = K_{5/3} + dK_{2/3}/dx = (1/2)(K_{5/3} - K_{1/3}),$$

$$F_{\sigma} = K_{5/3} - dK_{2/3}/dx = (1/2)(3K_{5/3} + K_{1/3}),$$

K_{ν} is the Macdonald function.

Formulas (1) contain the parameter q_a that determines the radiation mode. The parameter q_a is defined as the quotient of the acceleration of the particle motion in the small Larmor circle to the centrifugal acceleration due to movement on the larger circumference of radius equal to the radius of curvature of the magnetic field line. Also, it is the ratio of Larmor's speed $\omega_B r_B$ to the speed of centrifugal drift. This parameter indicates the extent of changing the curvature radius along the particle trajectory. Formula (1) has classical synchrotron or curvature radiation limits when $q_a \gg 1$ or $q_a \ll 1$, respectively [3, 4].

The parameter q_a can be written as

$$q_a = 1.5 \left(\frac{B}{2\text{T}} \right) \left(\frac{R}{200\text{cm}} \right) \left(\frac{40\text{MeV}}{E} \right) \left(\frac{\alpha}{0.05} \right),$$

where energies E are measured in MeV, magnetic field B is measured in T.

Equations (1) are valid for arbitrary values of the parameter q_a . Formula (1) should be used whenever the parameter value of the order of unity, $q_a \sim 1$. In other cases, the classical formulas of synchrotron radiation can be applied.

Taking sum of components $F = F_\pi + F_\sigma$ in eq. (1) we obtain the formula of total spectral power. Then, the formula obtained and eq. (15) in [5] corresponds to each other (more details see in [4]).

In Fig. 1, the spectra of total emitted power ($F = F_\pi + F_\sigma$ in eq. (1)) for different particle energies E and pitch angles α are shown. The vertical lines show the range of wavelengths of visible light and infrared wavelengths. The magnitude of magnetic field is $B = 2 \cdot 10^4$ G. The radiated power increases in magnetic field $B = 3 \cdot 10^4$ G.

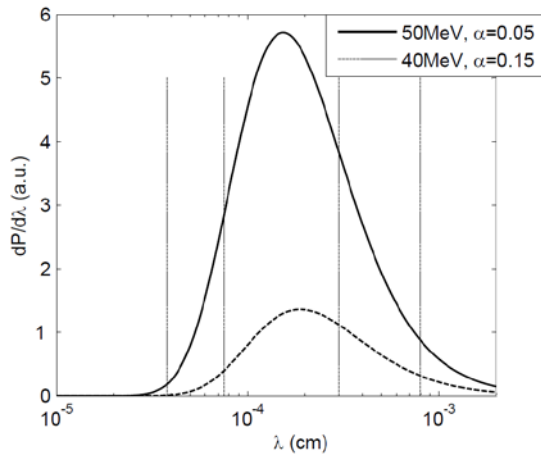


Fig. 1. Spectra according eq. (1): magnetic field $B = 2 \cdot 10^4$ G, curvature radius $R_B = 180$ cm. Radiation bands: visible light $0.38 \dots 0.75 \mu\text{m}$ (left) and infrared wavelength $3 \dots 8 \mu\text{m}$ (right)

2. TOROIDAL MAGNETIC FIELDS AND ELECTRON TRAJECTORIES

Cartesian coordinates are taken as shown in Fig. 1. The torus is described with coordinates (r, ϑ, φ) : coordinates (r, ϑ) with centre at major radius R and the toroidal angle φ , $\mathbf{e}_r, \mathbf{e}_\vartheta, \mathbf{e}_\varphi$ are the corresponding oris, $\mathbf{e}_\varphi = [\mathbf{e}_r, \mathbf{e}_\vartheta]$. Magnetic surfaces and drift surfaces have a toroidal topology. The major radius of nested magnetic surfaces is $R = R_0$, the major radius of drift surfaces is $R = R_0 + \delta$.

So, there are two coordinate systems (r, ϑ, φ) and $(r_f, \vartheta_f, \varphi)$ corresponding to drift and magnetic torus, respectively.

Suppose, the toroidal magnetic field \mathbf{B}_φ and plasma current \mathbf{I} are clockwise, radiating electrons are moving counterclockwise.

Magnetic fields take the form [11]

$$\mathbf{B}(r, \vartheta) = \frac{-B_0}{1 - r \cos \vartheta / R_0} \left[\frac{r}{q(r)R_0} \mathbf{e}_\vartheta + \mathbf{e}_\varphi \right], \quad (2)$$

here $r = r_f, \vartheta = \vartheta_f$ are the radius and poloidal angle of magnetic surface, $q(r)$ the safety factor. The subscript f is omitted in eq. (2).

Suppose that the safety factor of the magnetic field lines $q(r_f)$ is equal that of the particle drift orbits $q_D(r)$ when equal radii of magnetic field line surface r_f and drift surface r are considered [7].

The guiding center is moving along drift trajectory with speed v_\parallel . The electron pitch angle is $\alpha \approx v_\perp / v_\parallel \ll 1$, where $v_\perp = \omega_B r_B$, $\omega_B = eB / (\gamma mc)$, $B = B(r, \vartheta)$ the magnetic field at the point with drift coordinates r, ϑ .

The electron velocity vector is given by

$$\mathbf{v} = v_\parallel \boldsymbol{\tau}_D + v_\perp (-\sin \Theta \mathbf{v}_D - \cos \Theta \mathbf{b}_D), \quad (3)$$

here $\boldsymbol{\tau}_D, \mathbf{v}_D, \mathbf{b}_D$ are the tangent, normal, and binormal to the drift path, the angle Θ is measured from normal \mathbf{v}_D to the direction of vector $-\mathbf{b}_D$, $\dot{\Theta} = \omega_B$ (Fig. 2).

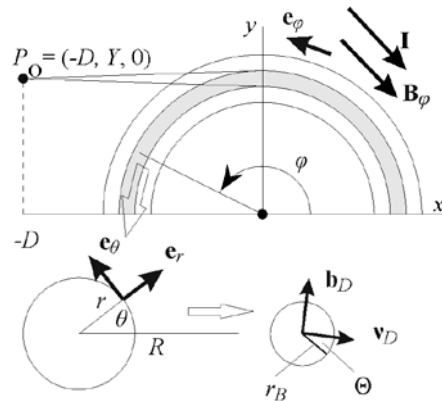


Fig. 2. Coordinate systems on torus. Cartesian coordinates (x, y, z) ; oris on a small circle of the torus $\mathbf{e}_r, \mathbf{e}_\vartheta, \mathbf{e}_\varphi$ (bottom left corner); Larmor's circumference and trihedron oris of the drift trajectory $\boldsymbol{\tau}_D, \mathbf{v}_D, \mathbf{b}_D$ (bottom right corner)

2.1. RADIATION POINTS

The detector is located at the point P_O with Cartesian coordinates $(-D, Y, 0)$ (see Fig. 2). The line of sight is directed from the detection point P_O to the radiation point P_e , denote unit vector in the direction $P_O P_e$ as \mathbf{n} . The high energetic electrons emit their synchrotron radiation practically along their velocity vector (3).

The coordinates of radiation point are founded out after equating components $-n_y, -n_z$ to the directional cosines of velocity vector, i. e., equations $\mathbf{v}\mathbf{n} + \mathbf{v} = 0$ are solved.

For any r, ϑ the third coordinate of radiation point takes a value $\varphi = \pi/2 + \Delta\varphi$, where $\Delta\varphi$ is the first-order correction with respect to $r/R \ll 1$, $\alpha \ll 1$.

The electron position in Larmor circle, angle Θ , is given by [6]

$$\cos \Theta = \frac{r}{\alpha q_D(r) R \cos \vartheta_0} \cos(\vartheta - \vartheta_0), \quad (4)$$

where $\cos \vartheta_0 = D / \sqrt{D^2 + (q_D R)^2}$.

From equation $v_y + \nu n_y = 0$ follows

$$\Delta\varphi = -\frac{Y - R + r \cos \vartheta}{D} + \frac{r}{q_D R} \cos \vartheta - \alpha \sin \Theta, \quad (5)$$

$q_D(r) = (n+1)q_0 \frac{r^2/a^2}{1 - (1 - r^2/a^2)^{n+1}}$ models the safe factor of drift path, $n=1..7$, a is the small tokamak radius [11]. Larmor radius r_b is not taken into account because of its smallness. (see also, eqs. (14), (15) in [10])

The range of angles ϑ depends on pitch-angles α . As can see from eq. (4), there are constraints on acceptable angles ϑ when $\alpha < r/(q_D R_D \cos \vartheta_0)$.

The shift δ of the drift trajectory is given by [7, 10]

$$\delta(r) = q(r) \gamma mc^2 / (eB). \quad (6)$$

Using this formula, one can model dependence of δ on the radius r .

2.2. PARAMETERS FOR SYNCHROTRON RADIATION FORMULAS

Available coordinates (r, ϑ, φ) of the guiding center of electron are given by (4), (5). At the point, the curvature radius $R_D(r, \vartheta, \varphi)$ of the drift trajectory is calculated. Then, the radius R_B is replaced by $R_D(r, \vartheta)$ in formula (1). Further, the value $B(r, \vartheta)$ of magnetic field is found at this point.

The parameter q_a can be written as

$$q_a = \frac{e}{mc^2} B(r_f, \vartheta_f) R_D(r, \vartheta) \frac{\alpha}{\gamma}, \quad (7)$$

where $R_D = R_0 + \delta + \left(-1 + \frac{1}{q_D^2}\right) r \cos \vartheta$ is the curvature radius of drift trajectory in a first-order approximation.

To calculate the magnetic field at the point $P_e = \left(r, \vartheta, \frac{\pi}{2}\right)$ the displacement in equatorial plane of the drift torus with respect to magnetic torus is taken into account, then $r_f = \sqrt{r^2 + \delta^2 - 2\delta r \cos \vartheta}$ and $\cos \vartheta_f = \frac{r \cos \vartheta - \delta}{r_f}$. Therefore, the magnetic field value is expressed by

$$B = B_0 \left(1 + \frac{r \cos \vartheta - \delta}{R_0}\right). \quad (8)$$

In Fig. 3, the total radiated power is shown. Note that the maximum (white color) and minimum (black color) values differ by 16 times.

An inclination angle of the radiation spot is given by (4) and is $\pi/2 + \vartheta_0$ (measured in the poloidal plane in such way as angle ϑ). If the drift trajectory is wound in opposite direction ($-\mathbf{e}_\vartheta$ direction), one obtains a mirror image relative to axis Oy . In this case, the inclination angle is $\pi/2 - \vartheta_0$.

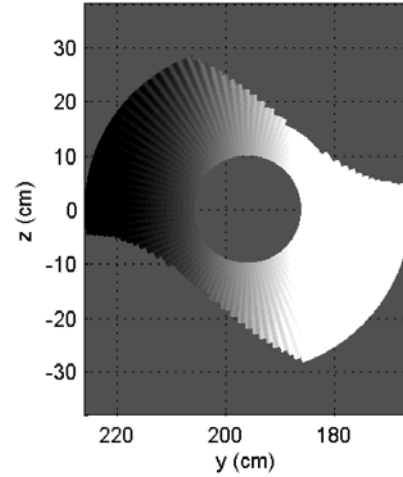


Fig. 3. Total radiated power at the wavelength $\lambda=0.5 \mu\text{m}$; $R_0=186 \text{ cm}$; $\delta=10 \text{ cm}$; $r=10..30 \text{ cm}$; $D=186 \text{ cm}$; $B_0=2 \cdot 10^4 \text{ G}$; $\alpha=0.12$; $E=40 \text{ MeV}$; $q_0=1$; $n=2$; $a=45 \text{ cm}$

We can say that the figure 'explains' the experimentally observed synchrotron spot [8] Fig. 12; [9] Fig. 6.

2.3. POLARIZATION VECTOR

As known, the direction of the larger axis of polarization ellipse for synchrotron emission of relativistic electrons moving on a circular orbit coincides with the direction of particle's acceleration [12]. Let χ be an angle between the axis Oz and the electron acceleration \mathbf{a} . Taking into account the smallness of angle between the line of sight and axis Ox , we find that $\sin \chi = \frac{a_y}{a}$, $\cos \chi = \frac{a_z}{a}$. The acceleration is found as the vector sum of the acceleration due to movement along drift trajectory and the acceleration owing to Larmor rotation.

Then

$$\sin \chi = \frac{-1 + q_a \cos \Theta - \left(b \cos \vartheta + b_1 \frac{q_a}{q_D} \sin \vartheta \sin \Theta\right)}{\sqrt{1 + 2b \cos \vartheta - 2q_a(1 - b \cos \vartheta) \cos \Theta + q_a^2}}, \quad (9)$$

and

$$\cos \chi = \frac{q_a \sin \Theta - \frac{b_1}{q_D} (1 - q_a \cos \Theta) \sin \vartheta}{\sqrt{1 + 2b \cos \vartheta - 2q_a(1 - b \cos \vartheta) \cos \Theta + q_a^2}}, \quad (10)$$

where $b_1 = \frac{r}{q_D(r) R_D(r, \vartheta)}$, $b = b_1 \cdot \left[q_D(r) - \frac{1}{q_D(r)}\right]$.

To describe the polarization properties we use the Stokes parameters I, Q, U, V . According ([12] eq. (5.28))

$$I \propto \frac{dP_\sigma}{d\lambda} + \frac{dP_\pi}{d\lambda},$$

$$Q \propto \left(\frac{dP_\sigma}{d\lambda} - \frac{dP_\pi}{d\lambda} \right) \cos 2\tilde{\chi},$$

$$U \propto \left(\frac{dP_\sigma}{d\lambda} - \frac{dP_\pi}{d\lambda} \right) \sin 2\tilde{\chi},$$

where $\tilde{\chi} \in (0, \pi)$ is the angle between some arbitrary fixed direction, axis $0z$ in our case, and the major axis of the ellipse of polarization. The angle is measured clockwise from the selected direction. The homogeneity of the electron distribution function implies that $V = 0$.

2.4. ONE OR TWO EMISSION POINTS ?

It follows from (4) that each \mathcal{G} corresponds to two values of Θ . Substituting them into (5) we get two values of the angle φ . It turns out that electrons radiate from two different places.

We add up Stokes parameters for these two emitting points, $Q = Q_1 + Q_2$, $U = U_1 + U_2$. Expressions (9), (10) are substituted for $\sin \tilde{\chi}$, $\cos \tilde{\chi}$ in trigonometric formulas for doubled angles.

Then the degree of polarization is defined as [12]

$$\pi(\lambda) = \frac{\sqrt{Q^2 + U^2}}{I}, \quad (11)$$

and angle $\tilde{\chi}$

$$\text{tg } 2\tilde{\chi} = \frac{U}{Q}. \quad (12)$$

By definition, the angle $\tilde{\chi}$ describes the direction in the picture plane in which the intensity of the polarized components has maximum.

Using Eqs. (3)-(12) we will calculate the distributions of the total intensity I , degree of polarization π and polarization directions $\tilde{\chi}$ in the synchrotron radiation spot from a homogenous electron beam with radius $r \in [r_{\min}, r_{\max}]$. If $\delta = \delta(r)$, $Y = R_0 + \delta(0)$ is taken.

3. DISCUSSION

The monoenergetic distribution function and a given pitch angle are supposed [7 - 10]. The distribution is also homogenous in space.

The formula (1) of synchrotron radiation in curved magnetic fields is valid for arbitrary values of parameter q_a .

The distribution of total intensity in the area of synchrotron spot is shown in Fig. 3. The radiation point coordinates are plotted in (y, z) -plane. The color (gray colormap) shows the radiation power (in arbitrary units) at a given wavelength λ (in this case, the wavelength $\lambda = 0.5 \mu\text{m}$). The parameters for calculations are taken as in the middle-sized tokamaks [7 - 10].

The power emitted at a given spot point depends strongly on the values of α and γ . In Fig. 3 we see that the radiation is stronger in the area of larger magnetic fields (closer to axis z) than in the area with smaller magnetic field (further from axis z).

This dependence may be the cause of the observed heterogeneity in the synchrotron radiation spots ([8] Fig. 12; [9] Fig. 6).

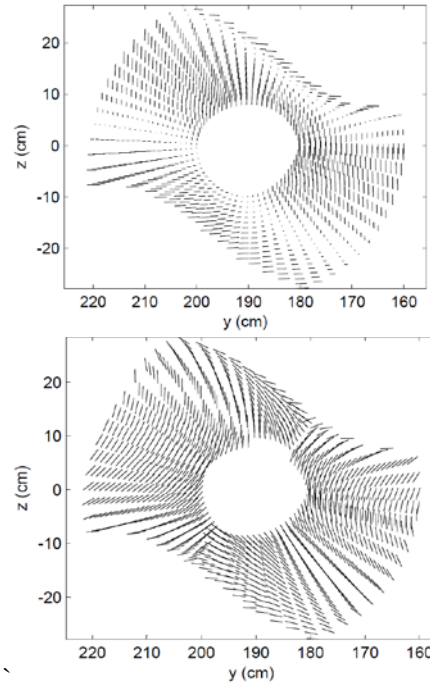


Fig. 4. Polarization of the synchrotron spot (poloidal projection) at the wavelength $\lambda = 5 \mu\text{m}$. Parameters: $B_0 = 2 \cdot 10^4 \text{ G}$, $E = 50 \text{ MeV}$, $\alpha = 0.12$, $r = 10 \dots 30 \text{ cm}$, $R_0 = 180 \text{ cm}$, $\delta = 10 \text{ cm}$, $D = 186 \text{ cm}$, $q_0 = 1$, $n = 2$, $a = 45 \text{ cm}$

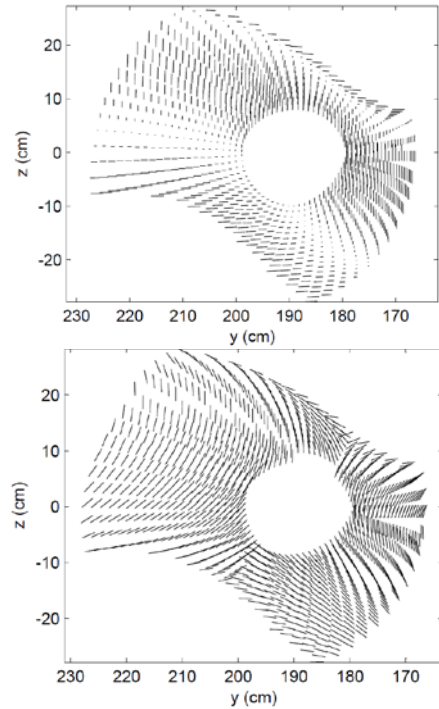


Fig. 5. Polarization of the synchrotron spot with drift trajectories shift $R_0 + \delta(r)$ at the wavelength $\lambda = 5 \mu\text{m}$ the values of $\delta(r)$ are given by (6): $q_0 = 1$, $n = 2$, $a = 45 \text{ cm}$. Other parameters as in Fig. 4

At different values of the given (experimental) parameters, the parameter q_a often takes value near unity that evidenced in favor of using Eqs. (1).

The directions of polarization in the synchrotron radiation spot are shown in Fig. 4. The length of dashes is proportional to the degree of polarization. Two models have been taken to calculate the polarization. In the upper part of the figure, a case when the contribution to

the polarization comes from two emission points has been considered. The degree of polarization varies from 0 to 72%. This range of values depends on α and γ . Polarization directions are orthogonal.

The lower part of the figure shows the case when the radiation comes from a single point (as it discussed in subsection 3.4). The absolute value of the degree of polarization is almost unchanged. The degree of polarization is about 70%. The directions of polarization behave differently than in the upper part of the figure.

In the case of small pitch angles α the polarization directions are determined by accelerations of guiding center, i. e. by the normal vector to the drift trajectory (along axis y). For large α the polarization direction is generated by centrifugal accelerations within Larmor circle. This gives the direction along axis z .

In Fig. 5, as in [10], the displacement (6) of drift trajectories is taken into account. As in Fig. 4, the upper part of the figure shows the case with two radiating points from the given direction, but the lower part shows the case with contributions from a single point.

Upper parts in Figs. 4, 5 show polarization directions as well as areas of zero polarization. It should be noted the change of polarization direction on 90° .

Assume that a similar cause may be responsible for changing the direction of polarization in the emission of pulsars.

Thus the synchrotron radiation is polarized and the distribution pattern of polarization directions in the spot and the degree of polarization can give additional data for diagnostics of electron beams.

REFERENCES

1. K.S. Cheng, J.L. Zhang. General radiation formulae for a relativistic charged particle moving in curved magnetic field lined: The synchro-curvature radiation mechanism // *Astrophys. J.* 1996, v. 463, № 1, p. 271-283.
2. Ya.M. Sobolev. Drift trajectory and synchrotron radiation of an ultrarelativistic electron moving in magnetic field with curved force lines // *Problems of Atomic Science and Technology. Series "Plasma Electronics and New Acceleration Methods"*. 2000, № 1, p. 27-30. http://vant.kipt.kharkov.ua/ARTICLE/VANT_2000_1/article_2000_1_27.pdf
3. Ya.M. Sobolev. Influence of magnetic line curvature on spectrum and polarization of synchrotron radiation of a charged particle // *Radio Physics and Radio Astronomy.* 2001, v. 6, № 4, p. 277-290. <http://journal.rian.kharkov.ua/index.php/ra/article/view/868/731>
4. Ya.M. Sobolev. On the synchrotron radiation of ultrarelativistic electrons moving along curved spiral trajectory // *Problems of Atomic Science and Technology. Series "Plasma Electronics and New Acceleration Methods"*. 2003, №4, p. 197-202. http://vant.kipt.kharkov.ua/ARTICLE/VANT_2003_4/article_2003_4_197.pdf
5. I.M. Pankratov. Towards analyses of runaway electrons synchrotron radiation spectra // *Plasma Physics Reports.* 1999, v. 25, № 2, p. 145-148.
6. Ya.M. Sobolev. Polarization of synchrotron radiation from relativistic electrons moving within toroidal magnetic fields // *Problems of Atomic Science and Technology. Series "Plasma Electronics and New Acceleration Methods"*. 2013, v. 4, p. 108-111. http://vant.kipt.kharkov.ua/ARTICLE/VANT_2013_4/article_2013_4_108.pdf
7. I. Entrop, R. Jaspers, N.J. Lopes Cardozo, K.H. Finken. Runaway snakes in TEXTOR-94 // *Plasma Phys. Control. Fusion.* 1999, v. 41, p. 377-398.
8. Y. Shi, J. Fu, J. Li, Y. Yang, et al. Observation of runaway electron beams by visible color camera in the Experimental Advanced Superconducting Tokamak // *Rev. Sci. Instrum.* 2010, v. 81, p. 033506.
9. A.C. England, Z.Y. Chen, D.C. Seo, et al. Runaway Electron Suppression by ECRH and RMP in KSTAR // *Plasma Sci. Technol.* 2013, v. 15, p. 119-122.
10. R.J. Zhou, I.M. Pankratov, L.Q. Hu, et al. Synchrotron radiation spectra and synchrotron radiation spot shape of runaway electrons in Experimental Advanced Superconducting Tokamak // *Physics of Plasmas.* 2014, v. 21, p. 063302.
11. J. Wesson. *Tokamaks.* Oxford: "Clarendon Press". 2004, 762 p.
12. V.L. Ginzburg. *Theoretical physics and astrophysics.* M.: "Nauka", 1987, 488 p.

Article received 18.05.2015

СИНХРОТРОННОЕ ИЗЛУЧЕНИЕ И ЕГО ПОЛЯРИЗАЦИЯ ОТ УБЕГАЮЩИХ ЭЛЕКТРОНОВ В ТОРОИДАЛЬНОМ МАГНИТНОМ ПОЛЕ

Я.М. Соболев

Предлагаются формулы для описания синхротронного излучения (СИ) и его поляризации в тороидальных конфигурациях магнитного поля. Оценены излучаемая мощность и направления поляризации в пятне синхротронного излучения убегающих электронов с параметрами, характерными для токамаков средних размеров. Рассматриваются две модели формирования поляризации. Показано, что измерение поляризации СИ может быть дополнительным средством для диагностики излучающих релятивистских электронов.

СИНХРОТРОННЕ ВИПРОМІНЮВАННЯ ТА ЙОГО ПОЛЯРИЗАЦІЯ ВІД УТІКАЮЧИХ ЕЛЕКТРОНІВ У ТОРОІДАЛЬНОМУ МАГНІТНОМУ ПОЛІ

Я.М. Соболев

Пропонуються формули, які описують синхротронне випромінювання (СВ) та його поляризацію в тороїдальній конфігурації магнітного поля. Дані оцінки потужності випромінювання і напрям поляризації у плямі синхротронного випромінювання утікаючих електронів для токамаків середніх розмірів. Розглянуто дві поляризаційні моделі. Показано, що вимірювання поляризації СВ може слугувати додатковим засобом для діагностики релятивістських електронів.